ESR investigation of the $[Al]^0$ center in tetragonal GeO_2 †

M. Stapelbroek, R. H. Bartram, and O. R. Gilliam
Department of Physics and Institute of Materials Science, University of Connecticut, Storrs, Connecticut 06268

David P. Madacsi
Department of Physics, Pennsylvania State University, Shenango Valley Campus, Sharon, Pennsylvania 16146
(Received 11 August 1975)

γ-ray, x-ray, or uv irradiation of an Al-doped tetragonal GeO_2 single crystal at 77 K generates holelike centers in four inequivalent sites. The ESR spectrum for one of the sites consists of a six-line hyperfine pattern corresponding to the interaction of a single unpaired spin with an ^{27}Al (100% abundant, $I = 5/2$) nucleus. Symmetry considerations and the spin-Hamiltonian parameters show that the hole is localized in the $2p_z$ orbital of one of four (out of six) nearest-neighbor oxygen anions. Owing to the low point symmetry (C_s) at the trapped-hole lattice site, the $\vec{g}$, $\vec{A}$, and $\vec{Q}$ tensors have only one common principal axis, which lies along a [110] direction (the $\vec{z}$ axis). Spin-Hamiltonian parameters are: $g_{z'} = 2.0040 \pm 0.0002$, $g_{y'} = 2.0143 \pm 0.0002$, $g_{x'} = 2.0202 \pm 0.0002$, $A_{z''} = 4.51 \pm 0.05$, $A_{y''} = 3.57 \pm 0.05$, and $A_{x''} = 4.50 \pm 0.05$, where the $\vec{A}$ components are in units of 10^{-4} cm^{-1}. The axes $\vec{y}'$ and $\vec{y}''$ make angles of $11.6° \pm 0.5°$ and $36.6° \pm 1.0°$ relative to the [001] direction, respectively, and $\vec{z}' = \vec{z}'' = \vec{z}$. A point-ion crystal-field calculation provides support for the defect model. Characteristics of the optical absorption spectra for the center are predicted assuming transitions between $2p$ levels of the O^- ion.

I. INTRODUCTION

Radiation-induced paramagnetic defects in GeO_2 have been studied by several investigators. Weeks and Purcell[1,2] have observed various holelike and electronlike defects in irradiated powder samples of both hexagonal and tetragonal GeO_2, as well as in amorphous (glassy) samples of GeO_2. Garlick *et al.*[3] have observed an additional holelike defect in polycrystalline hexagonal and amorphous samples. The models proposed for these defects have all been of an intrinsic nature.

We have previously reported the observation by electron-spin resonance (ESR) of a holelike defect associated with an Al impurity in hydrothermally grown single crystals of tetragonal GeO_2 following a low-temperature x-ray irradiation.[4] Recent success in the growth of Al-doped crystals using a flux method similar to those described by Swets[5] and Goodrum[6] has greatly enhanced the signal strength, enabled us to confirm its association with the Al impurity, and led to an improved model for this defect.[7] In brief, the model, which we label as the $[Al]^0$ center, corresponds to a hole localized on an oxygen ion adjacent to the Al^{3+} impurity ion. Similar centers, labeled as $[Ga]^0$ and $[In]^0$ centers in Ga- and In-doped crystals, will be discussed in a subsequent publication.[8]

Much work has been reported on Al^{3+} impurities in the isomorphic compound TiO_2 (rutile). Yahia[9] studied the electrical conductivity and thermoelectric power of Al-doped rutile. Several paramagnetic centers in slightly reduced (oxygen-deficient) TiO_2 containing Al impurities were ascribed to defect complexes involving both an interstitial and a substitutional Al^{3+} ion near a Ti^{3+} ion by Kerssen and Volger.[10] However, to our knowledge, trapped-hole centers associated with trivalent Al impurities, of the type we discuss here, have not been reported in the other rutile-structure oxides.

Trapped holes localized at O^{2-} sites adjacent to charge-deficient cation sites have been identified in many other oxide materials. Various types of V centers and the $[X]^0$ centers,[11] where X denotes an alkali-impurity cation, have been observed in the alkaline-earth oxides. Gamble *et al.*[12] have ascribed a component of the ESR spectrum of γ-irradiated Al_2O_3 to a hole trapped on an anion adjacent to an Al^{3+} vacancy or a charge-deficient cation. A point-ion crystal-field calculation by Bartram *et al.*[13] was employed to compute optical absorptions for this O^- ion. The strength of the crystal field was adjusted to fit the ESR results, which enabled them to assign the observed 3.08-eV optical band to this trapped hole in Al_2O_3.

In α-quartz a trapped-hole center associated with substitutional Al^{3+} impurities has been well characterized. The initial works by Griffiths *et al.*[14,15] and O'Brien and Pryce[16,17] proposed a defect model of a hole trapped on an oxygen anion adjacent to the Al^{3+} impurity. Schnadt and Schneider[18] determined the electronic structure of the smoky-quartz color center and observed similar centers in Ga-doped quartz crystals. Other researches on Al-doped α-quartz include

those by Samoilovich *et al.*,[19] Schnadt and Räuber,[20] and Mackey *et al.*[21]

II. CRYSTAL STRUCTURE

Tetragonal GeO_2 exhibits the well-known rutile structure (D_{4h}^{14}) illustrated in Fig. 1. The unit cell contains two inequivalent cation sites that are related by a 90° rotation about the c axis. The cations reside at lattice sites with D_{2h} point symmetry and each is surrounded by a distorted octahedron of oxygen anions. For one cation site, four nearest-neighbor anions, labeled ($\bar{b}$), lie in the (110) plane and two anions, labeled ($\bar{a}$), lie in the ($\bar{1}10$) plane, while for the other cation site these planes are reversed. The point symmetry at the oxygen lattice sites is C_{2v} in the perfect crystal. The ($\bar{a}$) anions are slightly more distant from the Ge site than the ($\bar{b}$) anions; the Ge-O($\bar{a}$) distance is 1.902 Å while the Ge-O($\bar{b}$) distance is 1.872 Å in the perfect crystal. The angle ρ shown in Fig. 1 is 40.1°.[22]

III. EXPERIMENTAL DETAILS

Single crystals of tetragonal GeO_2 were obtained by slowly cooling a GeO_2-Na_2O flux nominally doped with 200- and 1500-ppm Al in the form of Al_2O_3. Crystals as large as $10\times 3\times 3$ mm^3 were obtained. The holelike center could be generated at liquid-nitrogen temperatures by 1-MeV-electron, ^{60}Co γ-ray, x-ray, or uv irradiation. All ESR measurements were made at 92 K using Varian E-3 and E-12 X-band spectrometers. Crystals were accurately oriented using a Laue x-ray back-scattering technique.

The resonance lines were extremely narrow, having a width of about 0.12 G between inflection points at 92 K. The onset of power saturation at this temperature was found to occur at less than 1.0 mW of incident microwave power. Thermal annealing of the defect was complete and irreversible after approximately 5 min at 170 K.

IV. RESULTS

The ESR spectra observed at 92 K following x-ray irradiation at liquid-nitrogen temperature are shown in Figs. 2 and 3 for $\vec{H}$ parallel to the [001] and [110] crystallographic directions, respectively, for a crystal grown from flux doped with 200-ppm Al. The corresponding ESR signals were much less intense in undoped crystals and much more intense in crystals nominally doped with 1500-ppm Al. Six-line hyperfine patterns of allowed transitions ($\Delta M_s = \pm 1$, $\Delta M_I = 0$) and smaller forbidden transitions ($\Delta M_s = \pm 1$, $\Delta M_I = \pm 1, 2$) are evident in Figs. 2 and 3. The observed six-line hyperfine pattern is characteristic of interaction of the unpaired spin with a 100% naturally abundant spin-$\frac{5}{2}$ nucleus. The enhancement of the ESR signal caused by Al doping is evidence that the hyperfine interaction is with an ^{27}Al nucleus. The experimentally determined orientation dependence of the allowed hyperfine lines in two major crystallographic planes is shown in Fig. 4.

The magnitude of the hyperfine splitting is characteristic of a transferred hyperfine interaction similar to that observed for Al-related defects in other oxides.[18,23] The spectrum is attributed to a hole trapped on an O^{2-} anion interacting with a

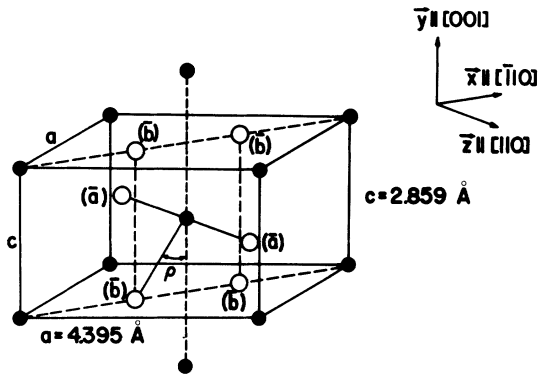

FIG. 1. Unit cell of tetragonal GeO_2 with the addition of two neighboring cations along the [001] direction. There are two inequivalent cation sites (dark circles) related by a 90° rotation about the c axis. The ($\bar{a}$) anions are at a slightly greater distance from the central cation than the ($\bar{b}$) anions. The Ge-O($\bar{b}$) bond direction makes an angle $\rho = 40.1°$ with the c axis.

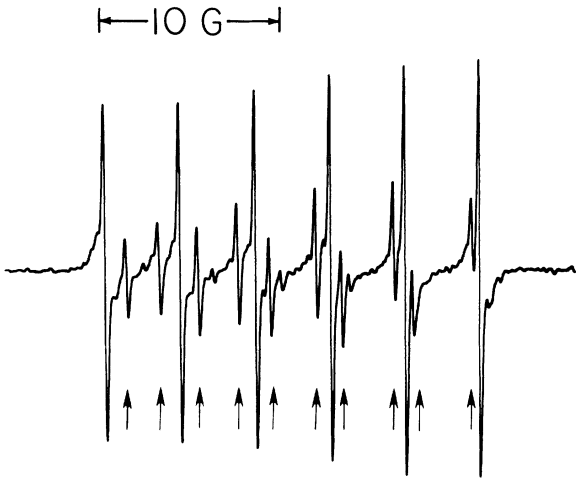

FIG. 2. ESR spectrum for $\vec{H} \| [001]$. The arrows indicate the $\Delta M_I = \pm 1$ forbidden transitions in between the six allowed hyperfine lines. The spectrum was recorded at 92 K and 9.2 GHz.

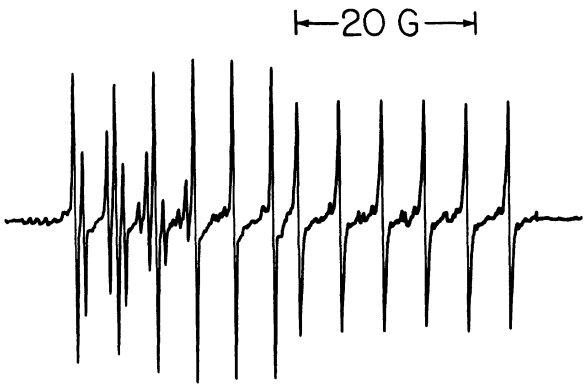

FIG. 3. ESR spectrum for $\vec{H} \| [110]$ showing two six-line hyperfine patterns. The high-field pattern does not exhibit $\Delta M_I = \pm 1$ forbidden transitions since it is due to centers aligned along the $\vec{z}$ axis, which is a principal axis for the quadrupole tensor. The spectrum was recorded at 92 K and 9.2 GHz.

nearby ^{27}Al nucleus. For an arbitrary orientation of the magnetic field, as many as four sets of six-line hyperfine patterns could be observed. This fact eliminated at least two possible models: (i) an Al^{3+} ion at a substitutional cation site interacting with a hole located on one of the two neighboring ($\bar{a}$) anions (this would result in at most two magnetically distinguishable sites); and (ii) a substitutional Al^{3+} ion interacting with a hole localized on ($\bar{a}$) and ($\bar{b}$) anions (this would result in a least six inequivalent sites). Furthermore, for $\vec{H}$ in the (001) plane of the crystal, only two sets of hyperfine lines could be observed, eliminating the possibility of an Al^{3+} ion at one of the known interstitial positions in the rutile lattice.[24] Therefore the spectrum was attributed to a hole localized on one of the four ($\bar{b}$) oxygen anions interacting with a substitutional Al^{3+} impurity ion.

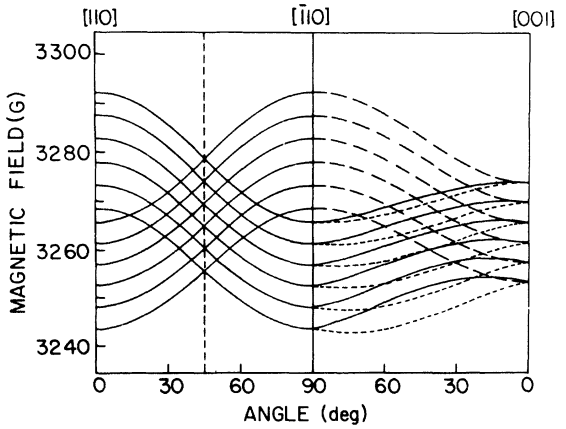

FIG. 4. Angular variation of the allowed hyperfine lines with rotation of $\vec{H}$ in the (001) and (110) planes. Two six-line hyperfine patterns corresponding to two magnetically inequivalent sites are observed in the (001) plane, and three are observed in the (110) plane.

The spin Hamiltonian appropriate to an $S = \frac{1}{2}$ defect including the hyperfine, quadrupole, and nuclear Zeeman interactions with one nucleus is

$$\mathcal{H} = \mu_B \vec{S}\cdot\bar{\bar{g}}\cdot\vec{H} + \vec{S}\cdot\bar{\bar{A}}\cdot\vec{I} + \vec{I}\cdot\bar{\bar{Q}}\cdot\vec{I} - g_N\mu_N\vec{H}\cdot\vec{I}. \quad (1)$$

In the unperturbed lattice the oxygen anions reside in sites that have orthorhombic (C_{2v}) point symmetry; however, the addition of a substitutional impurity ion lowers the symmetry of the ($\bar{b}$) anion sites to monoclinic (C_s), the only remaining symmetry element being the (110) mirror plane. This dictates that one of the principal axes for each of the $\bar{\bar{g}}$, $\bar{\bar{A}}$, and $\bar{\bar{Q}}$ tensors lies in the [110] direction ($\vec{z}$ axis). The directions of the other principal axes in the (110) plane are not constrained by symmetry, however, and indeed need not coincide.[25] The principal axes for the $\bar{\bar{g}}$, $\bar{\bar{A}}$, and $\bar{\bar{Q}}$ tensors are represented in Fig. 5 by single-, double-, and triple-primed axes, respectively.

Principal values of $\bar{\bar{g}}$ and $\bar{\bar{A}}$ and the angles α and β defined in Fig. 5 were obtained by a least-squares fit of the equations

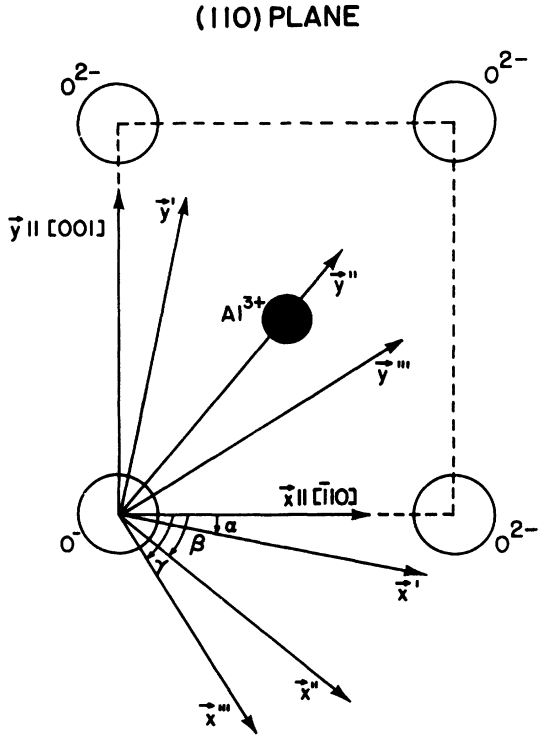

FIG. 5. Principal axes for the $\bar{\bar{g}}$, $\bar{\bar{A}}$, and $\bar{\bar{Q}}$ tensors of the spin Hamiltonian which are represented by single-, double-, and triple-primed axes, respectively.

TABLE I. Spin-Hamiltonian parameters for the [Al]^0 center in tetragonal GeO_2. The $\bar{A}$ tensor components are in units of $10^{-4}\,cm^{-1}$. The angles α and β, defined in Fig. 5, are in degrees.

$g_{x'}$	2.0202 ± 0.0002
$g_{y'}$	2.0143 ± 0.0002
$g_{z'}$	2.0040 ± 0.0002
α	11.6 ± 0.5
$A_{x''}$	4.50 ± 0.05
$A_{y''}$	3.57 ± 0.05
$A_{z''}$	4.51 ± 0.05
β	36.6 ± 1.0

$$g_{\rm eff}^2 = g_{x'}^2 \sin^2\theta \cos^2(\phi+\alpha) + g_{y'}^2 \sin^2\theta \sin^2(\phi+\alpha) + g_{z'}^2 \cos^2\theta$$

and (2)

$$A_{\rm eff}^2 = A_{x''}^2 \sin^2\theta \cos^2(\phi+\beta) + A_{y''}^2 \sin^2\theta \sin^2(\phi+\beta) + A_{z''}^2 \cos^2\theta$$

to the observed angular variation in the (110) plane, where ϕ and θ are the usual polar angles in the unprimed coordinate system. For these equations it is assumed that the skew-symmetric components of $\bar{g}$ and $\bar{A}$ are negligible; also, the equation for $A_{\rm eff}$ is a good approximation only if the anisotropy in $\bar{g}$ is small.[26] The center of the hyperfine pattern and the average separation were used to determine $g_{\rm eff}$ and $A_{\rm eff}$, respectively, at each orientation. Table I lists the tensor components and angles obtained.

Quadrupole tensor components were not precisely determined because their magnitudes are of the order of the uncertainty in the data. The directions of the principal axes of $\bar{Q}$ were found, however, by observing the disappearance of the $\Delta M_S = \pm 1$, $\Delta M_I = \pm 1$ forbidden transitions, which are presumed to disappear for $\vec{H}$ along principal directions of the quadrupole tensor.[27] The angle γ, defined in Fig. 5, was found to be $\gamma = 59° \pm 2°$. We estimated $|Q_i| < 0.2\times10^{-4}$ cm^{-1} for $i = x'''$, y''', or z'''.

V. CRYSTAL-FIELD CALCULATION

The introduction of an effective negative charge at the cation site occupied by the Al^{3+} impurity would lead us to expect a lower energy for a hole in an oxygen $2p$ orbital oriented along the Al^{3+} $-O^-$ bond direction. Instead, the nearly-free-electron value measured for the z component of $\bar{g}$ indicates that the trapped hole is localized mainly in a $2p_z$ orbital of the O^- ion. An *ab initio* point-ion crystal-field calculation was performed to clarify this result.

The point-ion crystal-field potential for an electron at an oxygen lattice site due to all the surrounding ions in the crystal can be expanded in terms of spherical harmonics by

$$V(\vec{r}) = -\sum_{L=0}^{\infty}\sum_{M=-L}^{L} e_{L,M} r^L Y_L^M(\theta,\phi), \tag{3}$$

where, in Slater atomic units,

$$e_{L,M} = \sum_{\alpha=0}^{\infty} \frac{8\pi Q_\alpha}{(2L+1) r_\alpha^{L+1}} Y_L^{M*}(\theta_\alpha, \phi_\alpha). \tag{4}$$

Here, Q_α is the charge on ion α, whose coordinates with respect to the origin are r_α, θ_α, and ϕ_α. Each term of Eq. (3), which is valid within the first spherical shell of ions, is a solution of Laplace's equation. The coefficients $e_{L,M}$ are constrained by symmetry; only combinations of spherical harmonics which transform as bases for the identity representation of the crystallographic point group at the anion site can contribute. The infinite lattice sums in Eq. (4) were evaluated by the method of Nijboer and deWette,[28,29] including the Al^{3+} defect contribution. Since terms in the expansion with $L > 2$ do not contribute to the matrix elements, the coefficients $e_{L,M}$ were calculated up to $L = 2$ and the nonvanishing coefficients are tabulated in Table II.

The ground state of O^- has the electronic configuration $1s^2 2s^2 2p^5$ with the excited configuration $1s^2 2s\, 2p^6$ lying 15.0 eV above the ground state in the free ion.[18] Using the unprimed coordinate system defined in Fig. 5, the $2s$, $2p_x$, and $2p_y$ orbitals transform as bases for the A' (identity) irreducible representation of C_s while $2p_z$ belongs to the A'' (antisymmetric) representation. The crystal field will not mix states belonging to different irreducible representations. The nonvanishing matrix elements of $-V$ are

$$\begin{aligned}
&\langle 2s|-V|2s\rangle = 1.103 \text{ a.u.},\\
&\langle 2p_x|-V|2p_x\rangle = \tfrac{1}{5}[(45/6\pi)^{1/2}\mathrm{Re}(e_{2,2}) - (5/4\pi)^{1/2} e_{2,0}]\langle r^2\rangle_{2p},\\
&\langle 2p_y|-V|2p_y\rangle = \tfrac{1}{5}[-(45/6\pi)^{1/2}\mathrm{Re}(e_{2,2}) - (5/4\pi)^{1/2} e_{2,0}]\langle r^2\rangle_{2p},\\
&\langle 2p_z|-V|2p_z\rangle = \tfrac{2}{5}(5/4\pi)^{1/2} e_{2,0}\langle r^2\rangle_{2p},\\
&\langle 2p_x|-V|2p_y\rangle = -(3/10\pi)^{1/2}\mathrm{Im}(e_{2,2})\langle r^2\rangle_{2p},\\
&\langle 2s|-V|2p_x\rangle = (1/2\pi)^{1/2}\mathrm{Re}(e_{1,1})\langle r\rangle_{2s2p},
\end{aligned} \tag{5}$$

and

$$\langle 2s|-V|2p_y\rangle = (1/2\pi)^{1/2}\mathrm{Im}(e_{1,1})\langle r\rangle_{2s2p}.$$

For these matrix elements the constant $L = 0$ term

TABLE II. Calculated crystal-field expansion coefficients for the $[Al]^0$ center in tetragonal GeO_2 (in a.u.).

$e_{0,0}$	5.008
$e_{1,1}=-e_{1,-1}^*$	$-0.074+i0.177$
$e_{2,0}$	-0.307
$e_{2,2}=e_{2,-2}^*$	$0.086+i0.043$

TABLE III. Calculated hole orbitals for the $[Al]^0$ center in tetragonal GeO_2.

$$\psi_0 = p_z$$
$$\psi_1 = (0.237)p_x + (0.968)p_y - (0.088)s$$
$$\psi_2 = (0.971)p_x - (0.239)p_y - (0.017)s$$
$$\psi_3 = (0.037)p_x + (0.082)p_y + (0.996)s$$

in the expansion has been neglected since we are only interested in the energy differences. The quantities $\langle r^2\rangle_{2p}$ and $\langle r\rangle_{2s\,2p}$ are defined as the radial integrals $\langle R_{2,1}|r^2|R_{2,1}\rangle$ and $\langle R_{2,1}|r|R_{2,0}\rangle$, respectively. Both the numerical wave functions given by Hartree, Hartree, and Swirles[30] and the analytic wave functions calculated by Clementi[31] were used in evaluating these radial integrals, with the results, in a.u.,

$$\langle r^2\rangle_{2p} = 3.04 \tag{6}$$

for both kinds of functions, and

$$\langle r\rangle_{2s2p} = 1.27$$

and (7)

$$\langle r\rangle_{2s2p} = 1.23$$

for the numerical and analytic wave functions, respectively. Diagonalization of the crystal-field matrix yielded the energy levels shown in Fig. 6 and the wave functions given in Table III.

VI. DISCUSSION

The results of the point-ion crystal-field calculation confirm that the hole is localized in an oxygen $2p_z$ orbital as illustrated in Fig. 7, even though the point-ion model neglects the effects of covalency and lattice distortion. We argue that the covalency effects are small whereas the lattice distortion is significant. The dominant contribution to covalent binding for the O^- ion is expected to involve the three nearest-neighbor metal ligands shown in Fig. 7. For an unpaired spin fully localized on the Al ion, i.e., in a $2p_z$ orbital of Al^{3+}, the anisotropic part of the hyperfine interaction, $A_z'' - \frac{1}{2}(A_x'' + A_y'')$, is calculated[32] to be about 0.2 cm^{-1}; however, the observed anisotropic hyperfine interaction is less than 1×10^{-3} cm^{-1}. Therefore, only a small fraction of the unpaired spin density is localized on the Al ligand. On the basis of preliminary observations of partially resolved ^{73}Ge (7.76% naturally abundant, $I=\frac{9}{2}$) hyperfine structure, covalency with the two nearest-neighbor Ge^{4+} ions is also believed to be small in magnitude. On this basis then, the assumption of an ionic model appears to be justified.

In Al_2O_3, Bartram *et al.*[13] found that the strength of the crystal field was very sensitive to small distortions of the lattice. For the present case, the introduction of the effective positive charge at an oxygen site would tend to produce an outward

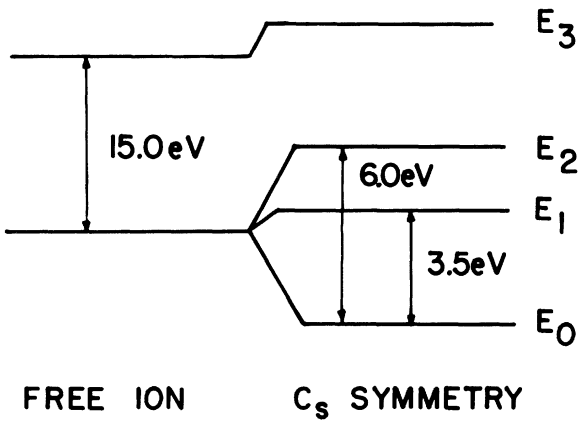

FIG. 6. Calculated energy levels for the $[Al]^0$ center in tetragonal GeO_2.

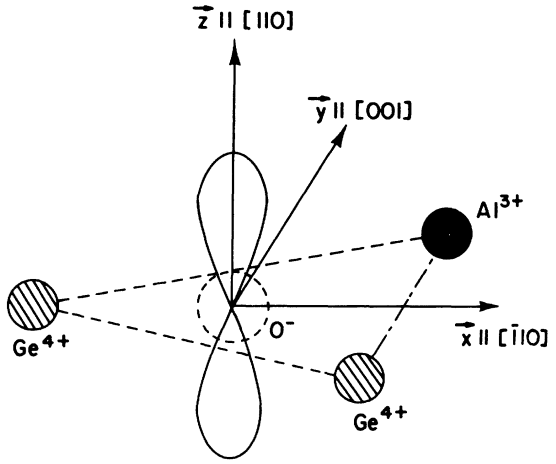

FIG. 7. Nearest-neighbor environment for the $[Al]^0$ center in tetragonal GeO_2. The hole is trapped in a p_z orbital of the O^- ion. The effective positive charge of the trapped hole is expected to cause an outward relaxation of the two Ge^{4+} ions from their normal lattice positions.

relaxation of at least the two nearest Ge^{4+} ions (see Fig. 7) with an expected reduction in the strength of the crystal field. Since we expect one of the principal axes of the hyperfine tensor to be along the Al^{3+}-O^- bond direction, direct experimental evidence of distortion may be seen in the result that this axis lies at an angle $\beta = 36.6° \pm 1.0°$. In the normal lattice the angle between the Ge^{4+}-O^{2-} bond, ρ, is 40.1°.

The reduction in the strength of the crystal field from that calculated assuming no lattice distortion may be seen by comparison of the observed and calculated principal g values. To first order, the deviations from the free-electron g value are given by[33]

$$\Delta g_{x'} = -2\lambda/(E_1 - E_0), \quad \Delta g_{y'} = -2\lambda/(E_2 - E_0),$$
$$\Delta g_{z'} = 0, \tag{8}$$

where λ is the spin-orbit coupling constant. For O^-, $\lambda = -135$ cm^{-1}, which was obtained by extrapolation from an isoelectronic sequence of ions.[13] A reduction in the calculated crystal-field potential by a factor of 2 would bring about good agreement between the calculated and experimental g shifts listed in Table IV. We believe this reduction is principally due to lattice distortion. The angle α shown in Fig. 5, representing the tilt of the $\tilde{g}$ tensor principal axes in the (110) plane, can be determined from the coefficients of ψ_1 as

$$\alpha = \arctan(C_{p_x}/C_{p_y}) = 13.8°, \tag{9}$$

which compares favorably to the measured value $\alpha = 11.6° \pm 0.5°$.

Two theories exist at present which attempt to explain the optical-absorption characteristics of trapped-hole centers in oxides. The older theory considers the optical bands as arising from transitions between the $2p$ levels of the O^- ion.[13] Although transitions between p states are forbidden by parity, this selection rule is relaxed because of admixture of the $2s$ orbital with the $2p$ orbitals via the crystal field. The optical transition energies are then simply related to the g values by Eqs. (8). This interpretation has been offered for the optical bands associated with trapped-hole centers in Al_2O_3[13] and MgO.[11] A more recent theory by Schirmer and co-workers[23,34] considers these trapped holes as bound small polarons and considers the optical absorption band to result from a charge transfer between adjacent oxygen anions. There is then no simple relation between optical and ESR results.

TABLE IV. Experimental and calculated deviations from the free-electron g value.

	Expt.	Calc.
$\Delta g_{x'}$	0.0179	0.0096
$\Delta g_{y'}$	0.0120	0.0056
$\Delta g_{z'}$	0.0017	0.0

Assuming transitions between $2p$ levels to be observable, we predict two optical bands corresponding to the transitions $\psi_0 \rightarrow \psi_1$ and $\psi_0 \rightarrow \psi_2$. With adoption of the factor of 2 reduction in the strength of the crystal field estimated from the g-shift data, the transition energies are expected to occur at about 1.8 and 3.0 eV (i.e., about half the calculated crystal-field splittings shown in Fig. 6). The bands will be dichroic; the transitions will occur only for light polarized along the $\tilde{z}$ axis of the defect. From the expected energies and calculated wave functions, the oscillator strengths for the transitions can be calculated from[35]

$$f_i = (E_i - E_0)|\langle\psi_i|z|\psi_0\rangle|^2, \tag{10}$$

where the energies are in rydbergs. This gives $f_1 = 6 \times 10^{-4}$ for the 1.8-eV band and $f_2 = 3 \times 10^{-5}$ for the 3.0-eV band. These approximate values for the oscillator strengths indicate that optical bands for the [Al]^0 center, arising from transitions between $2p$ levels, are weakly electric-dipole allowed, and should be observable if not obscured by other transitions.

VII. SUMMARY

We have observed and analyzed an ESR spectrum which occurs in Al-doped crystals of tetragonal GeO_2 following x-irradiation at liquid-nitrogen temperatures. The model we propose, designated the [Al]^0 center, consists of a substitutional Al^{3+} impurity ion interacting with a hole trapped on one of the four closest oxygens in the octahedron surrounding the impurity cation. A point-ion crystal-field calculation was performed and the electronic structure of the center was determined. The effects of covalency and distortion were discusse qualitatively and the expected characteristics of the optical absorption for the center were predicted, showing that transitions between $2p$ states of the O^- ion should be observable unless obscured by stronger bands.

ACKNOWLEDGMENTS

We acknowledge helpful discussions with Dr. L. A. Kappers and Dr. E. Kostiner. The computational portions of this investigation were performed at the University of Connecticut Computer Center.

†Supported by the University of Connecticut Research Foundation.

[1]R. A. Weeks and T. Purcell, J. Chem. Phys. 43, 483 (1965).
[2]R. A. Weeks, in *Recent Advances in Science and Technology of Materials*, edited by A. Bishay (Plenum, New York, 1974), Vol. I, p. 27.
[3]G. F. J. Garlick, J. E. Nicholls, and A. M. Özer, J. Phys. C 4, 2230 (1971).
[4]D. P. Madacsi and O. R. Gilliam, Bull. Am. Phys. Soc. 18, 467 (1973).
[5]D. E. Swets, J. Cryst. Growth 8, 311 (1971).
[6]J. W. Goodrum, J. Cryst. Growth 13/14, 604 (1972).
[7]M. Stapelbroek, O. R. Gilliam, and D. P. Madacsi, Bull. Am. Phys. Soc. 20, 376 (1975).
[8]T. J. Welsh, M. Stapelbroek, and O. R. Gilliam, Bull. Am. Phys. Soc. 20, 808 (1975).
[9]J. Yahia, Phys. Rev. 130, 1711 (1963).
[10]J. Kerssen and J. Volger, Physica (Utr.) 69, 535 (1973).
[11]A. E. Hughes and B. Henderson, in *Point Defects in Solids*, edited by J. H. Crawford, Jr. and L. M. Slifkin (Plenum, New York, 1972), Vol. 1, Chap. 7.
[12]F. T. Gamble, R. H. Bartram, C. G. Young, O. R. Gilliam, and P. W. Levy, Phys. Rev. 134, A589 (1964).
[13]R. H. Bartram, C. E. Swenberg, and J. T. Fournier, Phys. Rev. 139, A941 (1965).
[14]J. H. E. Griffiths, J. Owen, and I. M. Ward, *Report of the Bristol Conference on Defects in Crystalline Solids* (The Physical Society, London, 1954), p. 81.
[15]J. H. E. Griffiths, J. Owen, and I. M. Ward, Nature 173, 439 (1954).
[16]M. C. M. O'Brien and M. H. L. Pryce, *Report of the Bristol Conference on Defects in Crystalline Solids*, (The Physical Society, London, 1954), p. 88.
[17]M. C. M. O'Brien, Proc. R. Soc. A 231, 404 (1955).
[18]R. Schnadt and J. Schneider, Phys. Kondens. Mater. 11, 19 (1970).
[19]M. I. Samoilovich, L. I. Tsinober, V. E. Khadzhi, and M. V. Lelekova, Kristallografiya 13, 850 (1968) [Sov. Phys.-Crystallogr. 13, 734 (1969)].
[20]R. Schnadt and A. Räuber, Solid State Commun. 9, 159 (1971).
[21]J. H. Mackey, J. W. Boss, and D. E. Wood, J. Magn. Res. 3, 44 (1970).
[22]W. H. Baur and A. A. Khan, Acta Crystallogr. B 27, 2133 (1971).
[23]O. F. Schirmer, K. W. Blazey, W. Berlinger, and R. Diehl, Phys. Rev. B 11, 4201 (1975).
[24]H. J. Gerritson, in *Paramagnetic Resonance*, edited by W. Low (Academic, New York, 1963), Vol. I, p. 3.
[25]G. E. Pake and T. L. Estle, *The Physical Principles of Electron Paramagnetic Resonance* (Benjamin, Reading, Mass., 1973), p. 99.
[26]Reference 25, Chap. 5.
[27]A. Abragam and B. Bleaney, *Electron Paramagnetic Resonance of Transition Ions* (Clarendon, Oxford, England, 1970), p. 188. The derivation is given for axial symmetry only.
[28]B. R. A. Nijboer and F. W. de Wette, Physica (Utr.) 23, 309 (1957).
[29]F. W. de Wette and B. R. A. Nijboer, Physica (Utr.) 24, 1105 (1958).
[30]D. R. Hartree, W. Hartree, and B. Swirles, Philos. Trans. R. Soc. Lond. A 238, 229 (1939).
[31]E. Clementi, IBM J. Res. Dev. Suppl. 9, 2 (1965).
[32]M. Stapelbroek, T. J. Welsh, R. H. Bartram, and O. R. Gilliam (unpublished).
[33]C. P. Slichter, *Principles of Magnetic Resonance* (Harper and Row, New York, 1963), p. 183.
[34]O. F. Schirmer, P. Koidl, and H. G. Reik, Phys. Status Solidi B 62, 385 (1974).
[35]R. H. Dicke and J. P. Wittke, *Introduction to Quantum Mechanics* (Addison-Wesley, Reading, Mass., 1960), p. 276.